

# Novel Circularly Polarized SIW Cavity-Backed Antenna with Wide CP Beamwidth by Using Dual Orthogonal Slot Split Rings

Jian-Quan Huang<sup>1</sup>, Dajun Lei<sup>1</sup>, Chunzhi Jiang<sup>1</sup>, Zhenghua Tang<sup>1</sup>,  
Feng Qiu<sup>1, \*</sup>, Min Yao<sup>1</sup>, and Qing-Xin Chu<sup>2</sup>

**Abstract**—A circularly polarized (CP) substrate integrated waveguide (SIW) cavity-backed antenna based on dual concentric, orthogonal slot split ring resonators is proposed and experimentally studied. The circularly polarized wave is generated by two split ring-slots etched in the upper metal layer of the SIW cavity resonator. These two slots are excited by a coaxial probe located in the gap of the external slot split ring to radiate the right-handed circularly polarized (RHCP) wave. By rotating the dual split slot ring resonators and the probe by 45 degrees relative to the backed cavity, a better match characteristic and a slightly higher radiation gain are obtained. Because of the concentricity of radiant split ring slots, the beamwidth of the circular polarization is obviously increased. From the experimental results, the impedance bandwidth was 10.8% for the reflection coefficient less than  $-10$  dB, the axial ratio (AR) bandwidth was 1.54% for the AR less than 3 dB, and the RHCP gain was 4.44 dBic. Moreover, the 3-dB axial ratio beamwidth at the centre frequency of 10.40 GHz has been extended to  $142^\circ$  in the angular range from  $-78^\circ$  to  $+64^\circ$ .

## 1. INTRODUCTION

Cavity-backed circularly polarized (CP) antennas can reduce the multipath interferences, offer flexibility in orientation angle between receiving and transmitting terminals, have higher gain, and improve the electromagnetic compatibility/electromagnetic interference shielding and unidirectional radiation characteristic [1–4]. Hence, various waveguide cavity-backed CP antennas have been proposed for satellites, mobile communications and other wireless applications. However, the traditional waveguide cavity-backed CP antennas are also characterized by their bulky size, stringent manufacturing precision and high cost. To overcome these shortcomings, many substrate integrated waveguide (SIW) cavity-backed CP slot antennas have been proposed. The following three main radiating configurations of CP SIW cavity-backed slot antennas have been proposed in the literature: compound slots [5–9], annular, triangular or split ring slot [10–13] and patches, loop or cavity that cover the slots [14–19].

The pair of orthogonal straight slots etched on the SIW cavity can be excited to generate the CP circularly polarized wave [5, 6]. The cross-slots are similar to the compound orthogonal straight slot pair and can also realize the circular polarization [7, 8]. A circularly polarized radiating element consisting of four slots has been reported in [9], which can be considered a combination of the orthogonal slot pair. Another SIW cavity-backed CP structure is the annular [10, 11], triangular [12] or split ring [13] slot embedded in a cavity-backed resonator. The slot can radiate CP wave when dual orthogonal modes are excited in the SIW cavity resonator. In addition to the compound slots and ring slot etched on the SIW cavity, a rectangular strip rotated by an angle [14], a circular notched patch with stubs [15] or a truncated patch [16] that covers the SIW slot can be used to generate circular polarization. In [17],

---

Received 17 February 2017, Accepted 1 April 2017, Scheduled 12 April 2017

\* Corresponding author: Feng Qiu (jack8273193@163.com).

<sup>1</sup> School of Electronic Information and Electrical Engineering, Xiangnan University, Chenzhou, Hunan, China. <sup>2</sup> School of Electronic and Information Engineering, South China University of Technology, Guangzhou, China.

a rotated elliptical cavities fed by an SIW slot was used to radiate CP waves. Meanwhile, most of these works have concentrated on the miniaturization of the antenna, generation of CP radiation and enhancement of the 3-dB AR frequency bandwidth. However, the 3-dB axial ratio angular beamwidth is another key parameter of CP antennas that is as important as the aforementioned parameters. For example, in the flight control system for unmanned aerial vehicles (UAVs), a wider 3-dB axial-ratio (AR) beamwidth and a higher gain correspond to farther remote control distance. It is highly desired to explore these CP antennas with a wide 3-dB axial ratio angular beam-width.

Hence, the objective of this paper is to design a compact CP antenna with high gain and wide AR beamwidth. As shown in Figure 1, two orthogonal split ring slots etched on the SIW cavity are excited by a coaxial probe to generate a CP wave. Because of the concentricity of the dual split ring slots, a 3-dB AR/gain beamwidth of more than  $140^\circ$  and a gain of 4.44 dBic at boresight are obtained.

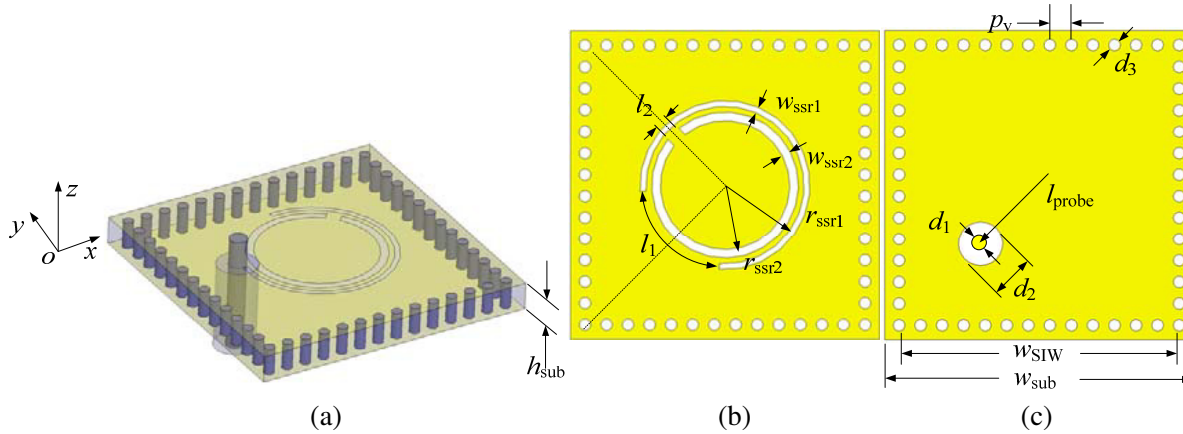


**Figure 1.** (a) Perspective view, (b) top view and (c) bottom view of the proposed antenna ( $p_v = 1.10$  mm,  $d_1 = 1.00$  mm,  $d_2 = 2.30$  mm,  $d_3 = 0.60$  mm,  $l_1 = 3.04$  mm,  $l_2 = 0.80$  mm,  $r_{ssr1} = 3.50$  mm,  $r_{ssr2} = 4.25$  mm,  $w_{ssr1} = 0.30$  mm,  $w_{ssr2} = 0.35$  mm,  $l_{probe} = 4.28$  mm,  $w_{SIW} = 14.50$  mm,  $w_{sub} = 16.00$  mm).

## 2. ANTENNA DESIGN

### 2.1. Circular-Polarization Mechanism

The design concept originates from the straight-slot antenna, which is illustrated in Figure 2(a). The polarized characteristic of the radiation wave is perpendicular to the slot. To miniaturize the antenna and facilitate the use of dual slots, the straight slot is bent to a split ring, whose radiation polarization is similar to the former, as shown in Figure 2(b). Therefore, two orthogonal split ring slots are arranged as shown in Figure 2(c) with perpendicular radiation polarizations. To obtain a good impedance match characteristic and high gain, the split ring slots are rotated by 45 degrees, and the fed probe is moved to the diagonal of the SIW cavity, as shown in Figure 2(d).

Figure 3 illustrates the electrical field distributions in dual orthogonal split ring slots that are etched on a cavity, which operated at 10.4 GHz with phase =  $0^\circ, 30^\circ, \dots, 330^\circ$ . Because of the orthogonal arrangement and coupling effect of two slots, the electrical distributions of the slots are no longer identical to the distribution of a single slot. Nevertheless, the sum electrical vector (the black arrow and solid line) of the inner (yellow arrow and dash line) and outer (red arrow and dot line) slots rotates in a counterclockwise direction with increasing phase. In other words, with the use of this arrangement, two orthogonal linearly polarized radiations are produced, and their linear superposition can be expected to achieve the desired circular polarization.

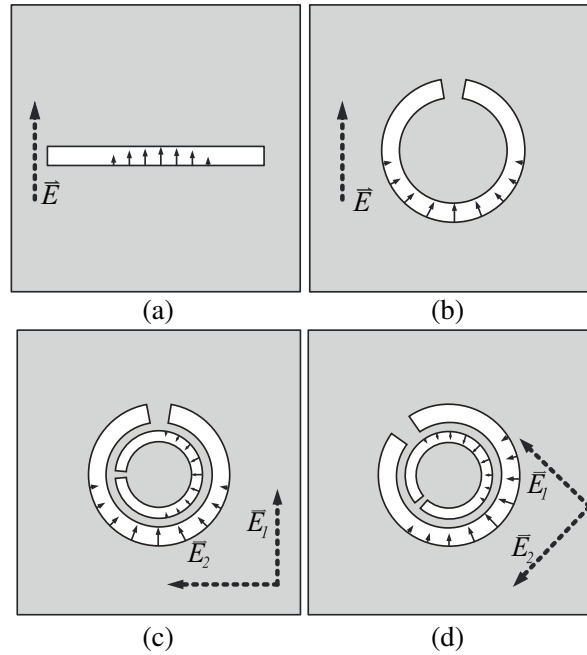


**Figure 2.** Electrical field in (a) a straight slot, (b) a split ring slot, (c) dual orthogonal split ring slots and (d) rotated dual orthogonal split ring slots by  $45^\circ$  in the cavity.

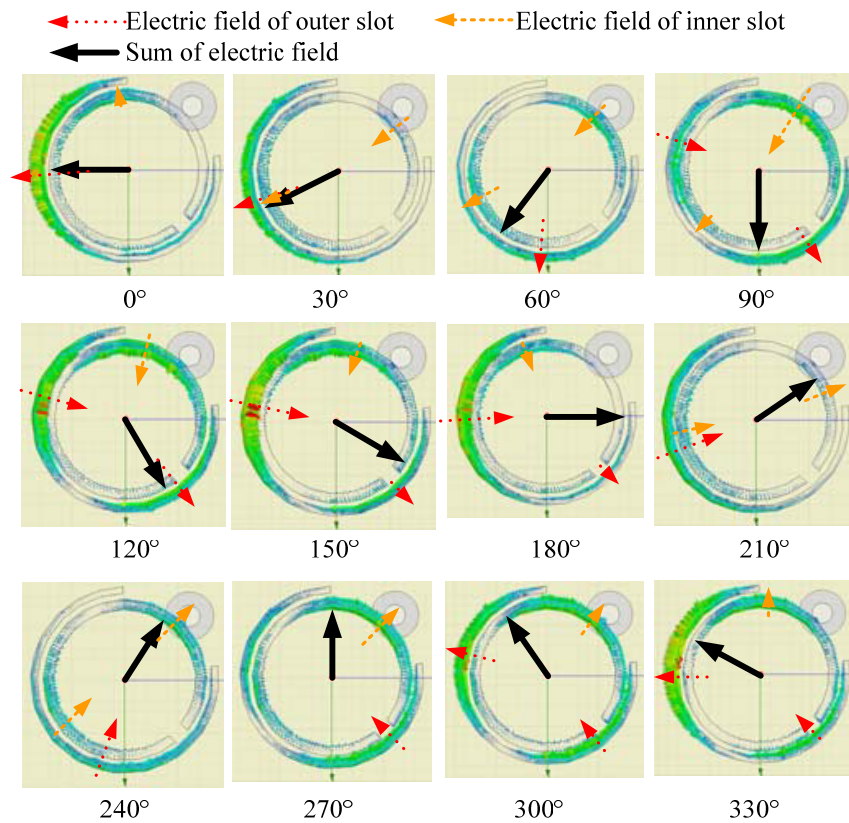


**Figure 3.** Electrical field distributions in the dual orthogonal split ring slots, which were etched on a cavity that operated at 10.4 GHz with phase =  $0^\circ, 30^\circ, \dots, 330^\circ$ .

## 2.2. Antenna Configuration

The configuration of the proposed antenna is illustrated in Figure 1. A square cavity with length  $w_{\text{SIW}}$  was created by four rows of vertical metallic vias arrays. The vias with diameter and distance of  $d_3$  and  $p_v$  penetrated through the substrate FR-4 PCB, whose width was  $w_{\text{sub}}$ , relative permittivity was 4.4, loss tangent was 0.02, and thickness was  $h_{\text{sub}} = 1.57$  mm. The external and internal split ring slots with diameters  $r_{\text{SRR1}}$  and  $r_{\text{SRR2}}$ , widths  $w_{\text{SRR1}}$  and  $w_{\text{SRR2}}$ , gap  $l_1$ , length  $l_2$ , respectively, were etched on the upper metal layer of the SIW cavity. The coaxial probe with diameters  $d_1$  and  $d_2$  of the inner and outer conductors is located in the gap of the external split ring slot with the distance of  $l_{\text{probe}}$  away from the centre of the SIW cavity.

## 2.3. Design Guidelines

As we know, the bandwidth of the cavity-backed antenna highly depends on the cavity substrate thickness and dielectric constant. In the design of the proposed antenna, after selecting the substrate according to the bandwidth, several initial geometries such as the lengths of the split ring slots and the size of cavity were determined by the operation frequency. Suppose that the antenna operates at frequency  $f$ ; the split ring slot and SIW cavity should resonate near this frequency. Consequently,  $f_{\text{slot}} \simeq f_{\text{SIW}} \simeq f$ , and the initiate values of the internal or external split ring slot can be estimated by resonate frequency  $f_{\text{slot}}$  as follows [20]:

$$f_{\text{slot}} = \frac{c}{2\pi \cdot r_{\text{SRR}} - l} \times \frac{1.25}{\sqrt{\varepsilon_{\text{eff}}}} \quad (1)$$

where  $c$  is the speed of light in free space;  $\varepsilon_{\text{eff}} = 2\varepsilon_r/(1 + \varepsilon_r)$  is the effective relative permittivity considering the presence of different dielectric media between the slot and the ground;  $r_{\text{SRR}}$  is the diameter of the external or internal slot ( $r_{\text{SRR1}}$  and  $r_{\text{SRR2}}$ );  $l$  is the length  $l_1$ ,  $l_2$  of the external or internal slot.

To design the square SIW cavity, the following two conditions must be considered:  $d_3 < 0.1\lambda_0$  and  $p_v < 2d_3$ , where  $\lambda_0$  is the free-space wavelength. The key parameter width  $w_{\text{SIW}}$  of the SIW cavity can be calculated using the resonant frequency  $f_{\text{SIW}}$  [21].

$$f_{\text{SIW}} = \frac{0.6c}{w_{\text{SIW}}\sqrt{\varepsilon_{\text{eff}}}} \quad (2)$$

where  $c$  and  $\varepsilon_{\text{eff}}$  are defined in Equation (1). After determining the initial geometries for the proposed antenna, a full-wave simulator HFSS is used to adjust the geometries to obtain a high-gain and CP radiation performance. According to the simulation results, all optimized dimensions of the proposed antenna are listed in Figure 1.

## 2.4. Parameter Study

The effects of key parameters on the AR at the broadside direction and reflection coefficient are analysed for further study. This provides a meaningful guideline for further practical design.

As illustrated in Figure 4(a), when  $l_2$  increases, the resonating frequency of the internal split ring slot moves to high frequency. Simultaneously, the 3-dB axial ratio bandwidth moves to a little higher frequency. The length  $l_1$  of the external slot has the identical effect on the operation frequency, as shown in Figure 4(b). However, when  $l_1$  or  $l_2$  varies too much, the axial ratio of the antenna may increase.

The dimension of the SIW cavity obviously affects the match characteristic and axial ratio of the antenna. When  $l_{\text{sub}}$  increases, the resonating frequency of the SIW cavity decreases, and the bandwidth of the antenna increases, but the reflection return loss and axial ratio increase, as shown in Figure 4(c).

The width of the split ring slots affects the axial ratio and return loss. As demonstrated in Figure 4(d), a larger width of the internal split ring slot corresponds with stronger radiation in the far field. Thus, the appropriate widths of the split ring slots contribute to the small axial ratio of the antenna. Meanwhile, a larger width will decrease the electric length of the split ring slot. As a result, the resonant frequency, bandwidth and return loss of the antenna will increase.

### 3. EXPERIMENTAL RESULTS AND DISCUSSION

A prototype of the proposed antenna has been successfully fabricated and tested to demonstrate the antenna's performances. The  $S$ -parameter of the proposed antenna was measured using the Agilent vector network analyser PNA N5230C, and the radiation characteristics were measured in a microwave chamber. The experimental results are consistent with the simulated ones compared in Figures 5–7.

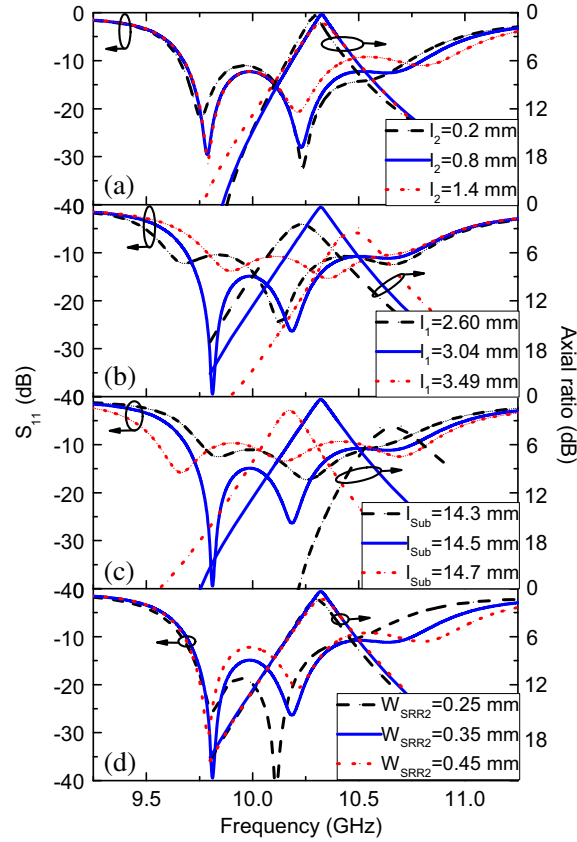


**Figure 4.** Effect of selected antenna parameters on the reflection coefficient and axial ratio: (a) width of  $l_2$ , (b)  $l_1$ , (c) size  $l_{sub}$  of the SIW cavity and (d) width  $W_{SRR2}$  of the internal split ring slot.

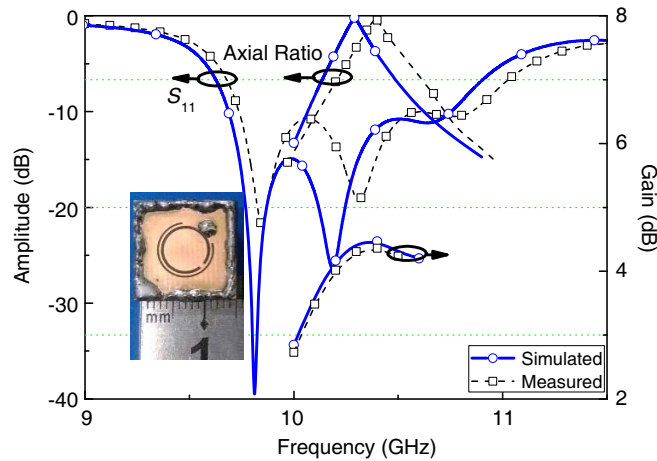


**Figure 5.** Measured and simulated reflect coefficients, axial ratios and gains of the proposed antenna.

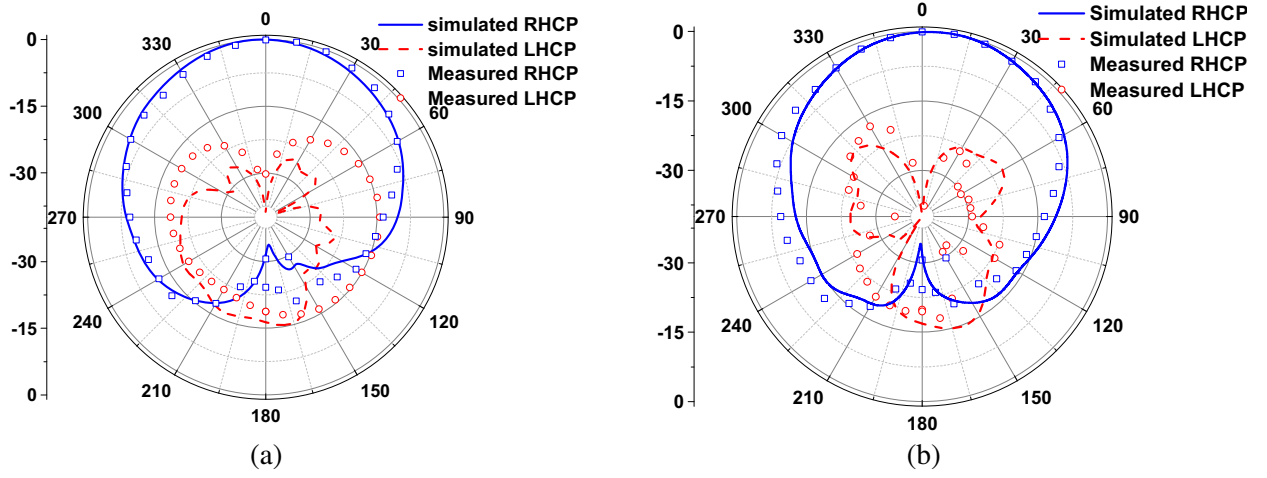


**Figure 6.** Measured and simulated 10.4 GHz normalized radiation patterns of orthogonal cut-planes for the fabricated antenna: (a)  $xoz$ - and (b)  $yo$ z-planes.

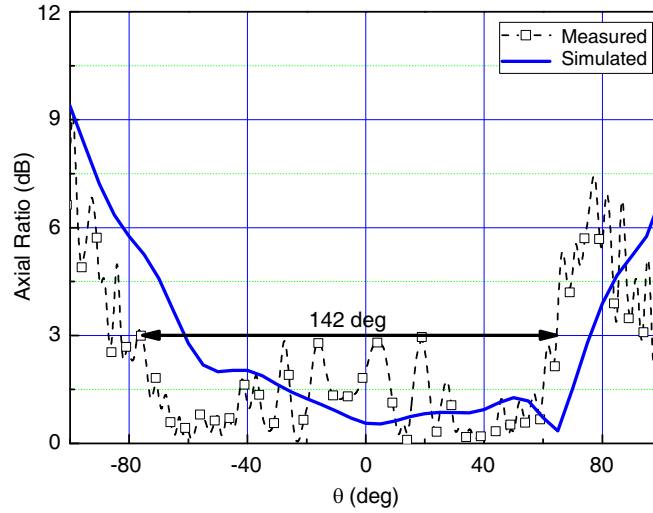


**Figure 7.** Measured and simulated axial ratios of the proposed antenna in the  $xoz$ -plane at 10.4 GHz.

The measured impedance bandwidth of 10.8% (for  $S_{11} < -10$  dB) is larger than the simulated one of 10.4%, as shown in Figure 5. The slight difference is mainly caused by the fabrication tolerances of some vital dimensions such as the width and length of the slots.

The proposed antenna has 4.4 dBic maximum RHCP measured realized gain at 10.0–10.6 GHz in the boresight direction (Figure 5), which is slightly smaller than the simulated value of 4.44 dBic. The simulated and measured results of the AR in the boresight direction ( $z$ -axis direction) versus frequency are also shown in Figure 5. The measured AR bandwidth is 1.5% (for  $AR < 3$  dB), which is slightly higher than the simulated value. The simulated and measured far-field radiation patterns in two orthogonal cutting planes at the frequency 10.4 GHz are depicted in Figure 6. It is proven that the antenna radiates an RHCP wave with broad beamwidth and low cross-polarization in the boresight direction.

Figure 7 depicts the simulated and measured axial ratios (ARs) as a function of the polar angle  $\theta$  at the central frequency 10.4 GHz of the proposed CP antenna. Both ARs are consistent over a wide angular range. Under the usual 3-dB AR definition, the measured AR beamwidth was 142°, i.e., from  $-78^\circ$  to  $64^\circ$ , which is slightly shifted by approximately  $12^\circ$  and slightly larger than the simulated value.

#### 4. CONCLUSIONS

In this paper, a notably compact X-band circularly polarized SIW back-cavity antenna has been proposed. Dual concentric, orthogonal slot split ring resonators were constructed in the SIW cavity, and the antenna exhibits a broad beamwidth and low cross-polarization in the boresight direction. The experimental results prove that the antenna had an impedance bandwidth of 10.8% (for  $S_{11} < -10$  dB), an AR bandwidth of 1.5% (for  $AR < 3$  dB), a realized RHCP gain 4.4 dBic and a 3-dB AR beamwidth of  $142^\circ$  in the boresight direction. The proposed configuration with the advantage of small size and light weight can be applied to wireless control systems such as the flight control system.

#### ACKNOWLEDGMENT

This work was supported by the Science and Technology Innovative Research Team in Higher Educational Institutions and the Research Foundation of Education Department (Grant No. 14C1061) of Hunan Province and Hunan Provincial Natural Science Fund (Grant No. 2016JJ4083).

#### REFERENCES

1. Montisci, G., M. Musa, and G. Mazzarella, "Waveguide slot antennas for circularly polarized radiated field," *IEEE Transactions on Antennas & Propagation*, Vol. 52, No. 2, 619–623, Feb. 2004.
2. Sze, J. Y. and W. H. Chen, "Axial-ratio-bandwidth enhancement of a microstrip-line-fed circularly polarized annular-ring slot antenna," *IEEE Transactions on Antennas & Propagation*, Vol. 59, No. 7, 2450–2456, Jul. 2011.
3. Karamzadeh, S., V. Rafii, H. Saygin, and M. Kartal, "Reconfigurable CP cavity back with ability to change polarisation diversity," *Electronics Letters*, Vol. 51, No. 25, 2080–2082, Dec. 2015.
4. Zhang, L., S. Gao, L. Qi, et al., "Single-feed ultra-wideband circularly polarized antenna with enhanced front-to-back ratio," *IEEE Transactions on Antennas & Propagation*, Vol. 64, No. 1, 355–360, Jan. 2016.
5. Chen, P., W. Hong, Z. Kuai, et al., "A substrate integrated waveguide circular polarized slot radiator and its linear array," *IEEE Antennas & Wireless Propagation Letters*, Vol. 8, No. 4, 120–123, Apr. 2009.
6. Sanchez-Olivares, P. and J. L. Masa-Campos, "Novel four cross slot radiator with tuning vias for circularly polarized SIW linear array," *IEEE Transactions on Antennas & Propagation*, Vol. 62, No. 4, 2271–2275, Apr. 2014.
7. Luo, G. Q., Z. F. Hu, Y. Liang, et al., "Development of low profile cavity backed crossed slot antennas for planar integration," *IEEE Transactions on Antennas & Propagation*, Vol. 57, No. 10, 2972–2979, Oct. 2009.
8. Elboushi, O. H. and A. Sebak, "High gain circularly polarized slot-coupled antenna for millimeter wave applications," *Microwave & Optical Technology Letters*, Vol. 56, No. 11, 2522–2526, Nov. 2014.
9. Hao, Z. C., X. Liu, X. Huo, et al., "Planar high gain circularly polarized element antenna for array applications," *IEEE Transactions on Antennas & Propagation*, Vol. 63, No. 5, 1937–1948, May 2015.
10. Jung, E. Y., J. W. Lee, T. K. Lee, et al., "SIW-based array antennas with sequential feeding for X-band satellite communication," *IEEE Transactions on Antennas & Propagation*, Vol. 60, No. 8, 3632–3639, Aug. 2012.
11. Guan, D. F., Y. S. Zhang, Z. P. Qian, et al., "Compact circular polarised SIW array antenna with high gain and conical-beam," *Electronics Letters*, Vol. 51, No. 24, 1962–1964, Nov. 2015.
12. Zhang, T., W. Hong, Y. Zhang, et al., "Design and analysis of SIW cavity backed dual-band antennas with a dual-mode triangular-ring slot," *IEEE Transactions on Antennas & Propagation*, Vol. 62, No. 10, 5007–5016, Oct. 2014.

13. Gharibi, H. and F. Hodjatkashani, "Design of a compact high-efficiency circularly polarized monopulse cavity-backed substrate integrated waveguide antenna," *IEEE Transactions on Antennas & Propagation*, Vol. 63, No. 9, 4250–4256, Sep. 2015.
14. Guntupalli, B. and K. Wu, "60-GHz circularly polarized antenna array made in low-cost fabrication process," *IEEE Antennas & Wireless Propagation Letters*, Vol. 13, No. 1933, 864–867, Apr. 2014.
15. Li, Y., Z. N. Chen, X. Qing, et al., "Axial ratio bandwidth enhancement of 60-GHz substrate integrated waveguide-fed circularly polarized LTCC antenna array," *IEEE Transactions on Antennas & Propagation*, Vol. 60, No. 10, 4619–4626, Oct. 2012.
16. Li, T., B. P. Wang, and W. B. Dou, "Substrate integrated waveguide slot array antenna covered by circularly polarised array patches," *Electronics Letters*, Vol. 51, No. 21, 1634–1635, Oct. 2015.
17. Lang, Y., S. W. Qu, and J. X. Chen, "Wideband circularly polarized substrate integrated cavity-backed antenna array," *IEEE Antennas & Wireless Propagation Letters*, Vol. 13, 1513–1516, Jul. 2014.
18. Xu, J. K., M. Wang, H. K. Huang, et al., "Circularly polarized patch array fed by slotted waveguide," *IEEE Antennas & Wireless Propagation Letters*, Vol. 14, 8–11, 2015.
19. Lu, L., Y.-C. Jiao, Z.-B. Weng, et al., "Design of low-sidelobe circularly-polarized loop linear array fed by the slotted SIW," *IEEE Antennas & Wireless Propagation Letters*, Vol. PP, No. 99, 1–1, Jul. 2016.
20. Chen, W. S., C. C. Huang, and K. L. Wong, "Microstrip-line-fed printed shorted ring-slot antennas for circular polarization," *Microwave & Optical Technology Letters*, Vol. 31, No. 2, 137–140, Aug. 2001.
21. Rao, J. S. and B. N. Das, "Impedance characteristics of transverse slots in the ground plane of a stripline," *Proc. IEE*, Vol. 125, No. 1, 29–32, Jan. 1978.